DYNAMIC SIMULATION OF FLIGHT TEST MANOEUVRES ON THE DIAMOND D-JET

Luc Van Bavel (Diamond Aircraft Industries, Canada); David M. Holman, Ruddy Brionnaud, María García-Camprubí (Next Limit Technologies, Spain)

Presented by David M. Holman, Head of XFlow Technology

THEME

Computational Fluid Dynamics

SUMMARY

The numerical simulation of the complex fluid-structure interaction taking place when manoeuvring an aircraft remains a challenge. A realistic analysis of the airplane manoeuvrability often involves the presence of moving parts, such as the deflection of the elevators, the ailerons, or the elevons. For conventional Computational Fluid Dynamics (CFD) codes, dealing with such moving geometries is a challenging task. The following work shows that this is not the case for XFlow (Next Limit Technologies, 2013), a novel CFD software based on the lattice-Boltzmann method.

This paper presents a numerical study on the dynamic simulation of flight test manoeuvres on the Diamond D-JET, using the XFlow virtual wind tunnel. The pitch capture manoeuvre is first simulated, studying the pitch oscillation response of the aircraft. Dutch roll flight mode is then numerically reproduced. Finally, the D-JET angle of attack is evaluated in the post-stall regime under controlled movements of the elevator.

Numerical results are eventually compared with the corresponding flight test data recorded by Diamond Aircraft Industries. Numerical and experimental results show a promising agreement. It may thus be concluded that: (i) XFlow can offer the opportunity to bypass some wind tunnel testing; and (ii) XFlow can complement flight tests by helping in mitigating risks associated with flight test manoeuvres, including fully developed stalls and spin testing.

KEYWORDS

DYNAMIC SIMULATION OF FLIGHT TEST MANOEUVRES ON THE DIAMOND D-JET

Lattice-Boltzmann method; CFD validation; aircraft flight dynamics; virtual flight testing; manoeuvring simulation.

1: Introduction

During the design stages of development for a new aircraft program, aerodynamic data are generally obtained from wind tunnel and flight tests. Wind tunnel experiments, though, may not be representative of some dynamic motions and its results may suffer from scalability issues. The main disadvantage of flight test data is that they are not available until late in the development process. In this context, CFD is considered as a promising tool to estimate aerodynamic data for flight manoeuvres at the early design stages. Numerical data is expected to greatly improve the efficiency and effectiveness of the flight test programs (Hines 2000).

In the literature, some CFD works on flight simulation consist in generating a tabular database of fundamental aerodynamic parameters, which are later used either to calculate static and dynamic stability derivatives, or as lookup tables by Six-Degree-of-Freedom simulations (e.g. Ghoreyshi et al. 2010, Lemon, K.A., 2011). The application of this classical two-step approach is limited since the aerodynamic forces and moments of an aircraft with high angle of attack and large amplitude manoeuvres, responding to sudden changes of the flow, depend on the time history of the motion. For instance, this approach particularly fails where post-stall motions or propeller slipstreams are considered.

More comprehensive CFD works on the simulation of dynamic manoeuvres consider the flow equations on dynamic meshes, e.g. Farhat et al. 2001. For conventional CFD codes, i.e. Eulerian approach, the handling of dynamic meshes requires a time-consuming remeshing process at each time step that often leads to numerical errors and convergence issues; thus being a challenge even for simplified geometries (e.g. Shishkin & Wagner, 2010; Johnson, 2006). However, this is not the case for XFlow (Holman et al. 2012), a novel CFD software based on the lattice-Boltzmann method, a kinetic approach to fluid dynamics combined with a set of adapting level of detail schemes which provide a smart solution for highly demanding applications.

The XFlow mesoscopic particle-based approach to CFD circumvents those moving-mesh issues, while its refinement algorithms allow the spatial discretization to be dynamically adjusted during the simulation, according to the wake structure. Hence, XFlow technology leads to an improvement of the overall accuracy and simultaneously to an efficient use of the computational resources.

DYNAMIC SIMULATION OF FLIGHT TEST MANOEUVRES ON THE DIAMOND D-JET

The ability of XFlow to conduct rigid body simulations concurrently with CFD analysis – including fully turbulent airflow cases – has been investigated as part of the ongoing research and development studies for the design of future aircraft at Diamond Aircraft Industries. To this end, XFlow has been used to dynamically simulate flight-test manoeuvres on the Diamond D-JET.

Figure 1: Diamond D-JET

The Diamond D-JET, shown in Figure 1, is a five-seat single engine jet currently undergoing flight testing in Canada. Its cruise speed is 315 knots (580 km/hr) and it is powered by the Williams FJ33-4A-19 turbofan engine. A sophisticated data acquisition system records hundreds of air data and systems parameters at high frequency. In addition to flight testing, the D-JET has also undergone wind tunnel testing at the University of Washington Aeronautical Laboratory (UWAL) in the US and at the Large Amplitude Multi-Purpose (LAMP) wind tunnel in Germany.

This paper presents the numerical results provided by XFlow for the D-JET dynamic manoeuvres and their comparison with the corresponding flight test data recorded by Diamond Aircraft Industries. Numerical results show a promising agreement with experimental data, indicating that XFlow capabilities in determining dynamic stability characteristics may offer the opportunity to bypass some wind tunnel testing. It is further concluded that XFlow may also complement flight test and help mitigate risks associated with several flight test manoeuvres, including fully developed stalls and spin testing.

2: Numerical approach

In the literature there are several particle-based numerical approaches to solve the computational fluid dynamics. They can be classified in three main categories: algorithms modelling the behaviour of the fluid at microscopic scale (e.g. Direct Simulation Montecarlo); algorithms which solve the equations at a macroscopic level, such as Smoothed Particle Hydrodynamics (SPH) or Vortex Particle Method (VPM); and finally, methods based on a mesoscopic framework, such as the Lattice Gas Automata (LGA) and Lattice Boltzmann Method (LBM).

The algorithms that work at molecular level have a limited application, and they are used mainly in theoretical analysis. The methods that solve macroscopic continuum equations are employed most frequently, but they also present several problems. SPH-like schemes are computationally expensive and in their less sophisticated implementations show lack of consistency and have problems imposing accurate boundary conditions. VPM schemes have also a high computational cost and besides, they require additional solvers (e.g. schemes based on boundary element method) to solve the pressure field, since they only model the rotational part of the flow.

Finally, LGA and LBM schemes have been intensively studied in the last years being their affinity to the computational calculation their main advantage. Their main disadvantage is the complexity to analyse theoretically the emergent behaviour of the system from the laws imposed at mesoscopic scale. XFlow approach to the fluid physics takes the main ideas behind these algorithms and extends them to overcome most of the limitations present on these schemes.

2.1 Lattice Gas Automata

The Lattice Gas Automata (LGA) is a simple scheme to model the behavior of gases. The basic idea behind the LGA is that particles with specific velocities (e_i, $i = 1. ..., b$) propagate through a d-dimensional lattice, at discrete times $t = 0, 1, 2, ...$ and collide according to specific rules designed to preserve the mass and the linear momentum when different particles reach the same lattice position.

The simplest LGA model is the HPP approach, introduced by Hardy, Pomeau and de Pazzis, in which particles move in a two-dimensional square lattice and in four directions ($d=2$, $b=4$). The state of an element of the lattice at instant t is given by the occupation number $n_i(\boldsymbol{r},t)$,with $n_i = 1$ being the presence and $n_i = 0$ absence of particles with velocity e_i.

The stream-and-collide equation that governs the evolution of the system is

$$n_i(\boldsymbol{r} + \boldsymbol{e_i}, t + dt) = n_i(\boldsymbol{r}, t) + \Omega_\mathrm{i}(n_i, \dots, n_b), \quad i = 1, \dots, b, \qquad (1)$$

where Ω_i is the collision operator that computes a post-collision state conserving mass and linear momentum. If one were to assume $\Omega_\mathrm{i} = 0$, only a streaming operation would be performed.

From a statistical point of view, the system is constituted by a large number of elements which are macroscopically equivalent to the problem investigated. The macroscopic density and linear momentum can be computed as:

$$\rho = \frac{1}{b}\sum_{i=1}^{b} n_i \tag{2}$$

$$\rho\boldsymbol{v} = \frac{1}{b}\sum_{i=1}^{b} n_i\,\boldsymbol{e_i} \tag{3}$$

2.2 Lattice Boltzmann method

While the LGA schemes use Boolean logic to represent the occupation stage, the LBM method makes use of statistical distribution functions f_i with real variables, preserving by construction the conservation of mass and linear momentum.

The Boltzmann transport equation is defined as follows:

$$\frac{\partial f_i}{\partial t} + e_i \cdot \nabla f_i = \Omega_{\mathrm{i}}, \qquad i = 1, \dots, b, \tag{4}$$

where f_i is the particle distribution function in the direction i, $\boldsymbol{e_i}$ the corresponding discrete velocity and Ω_{i} the collision operator.

The stream-and-collide scheme of the LBM can be interpreted as a discrete approximation of the continuous Boltzmann equation. The streaming or propagation step models the advection of the particle distribution functions along discrete directions, while most of the physical phenomena are modelled by the collision operator which also has a strong impact on the numerical stability of the scheme.

In the most common approach, a single-relaxation time (SRT) based on the Bhatnagar-Gross-Krook (BGK) approximation is used

$$\Omega_{\mathrm{i}}^{\mathrm{BGK}} = \frac{1}{\tau}\left(f_{\mathrm{i}}^{\mathrm{eq}} - f_{\mathrm{i}}\right), \tag{5}$$

where τ is the relaxation time parameter, related to the macroscopic viscosity as follows

$$\nu = c_s^2\left(\tau - \frac{1}{2}\right) \tag{6}$$

f^{eq}_i is the local equilibrium function usually defined as

$$f_i^{eq} = \rho w_i \left(1 + \frac{e_{i\alpha} u_\alpha}{c_s^2} + \frac{u_\alpha u_\beta}{2c_s^2}\left(\frac{e_{i\alpha} e_{i\beta}}{c_s^2} - \delta_{\alpha\beta}\right)\right). \qquad (7)$$

Here c_s is the speed of sound, $\boldsymbol{u}$ the macroscopic velocity, δ the Kronecker delta and the w_i are weighting constants built to preserve the isotropy. The α and β subindexes denote the different spatial components of the vectors appearing in the equation and Einstein's summation convention over repeated indices has been used.

By means of the Chapman-Enskog expansion the resulting scheme can be shown to reproduce the hydrodynamic regime for low Mach numbers (Ran & Xu, 2008; Qian et al. 1992; Higuera & Jiménez, 1989).

The single-relaxation time approach is commonly used because of its simplicity, however it is not well posed for high Mach number applications and it is prone to numerical instabilities.

Some of the BGK limitations are addressed with multiple-relaxation-time (MRT) collision operators where the collision process is carried out in moment space instead of the usual velocity space

$$\Omega_i^{\mathrm{MRT}} = \mathrm{M}_{ij}^{-1}\hat{\mathrm{S}}_{ij}\left(\mathrm{m}_i^{\mathrm{eq}} - \mathrm{m}_i\right), \qquad (8)$$

where the collision matrix $\hat{S}_{ij}$ is diagonal, $m^{eq}{}_i$ is the equilibrium value of the moment m_i and M_{ij} is the transformation matrix (Shan & Chen, 2007; d'Humières, 2002).

An alternative method that aims to overcome the limitations of the BGK approach is the entropic lattice Boltzmann (ELBM) scheme, which may rely on a single-relaxation-time where the attractors of the particle distribution functions are based on the minimization of a Lyapunov-type functional enforcing the H-theorem locally in the collision step. However, this method is expensive from the computational point of view (Asinari, 2008) and thus not used on practical engineering applications.

The collision operator in XFlow is based on a multiple relaxation time scheme. However, as opposed to standard MRT, the scattering operator is implemented in central moment space. The relaxation process is performed in a moving reference frame by shifting the discrete particle velocities with the local macroscopic velocity, naturally improving the Galilean invariance and the numerical stability for a given velocity set (Premnath & Banerjee, 2011).

Raw moments can be defined as

$$\mu x^k y^l z^m = \sum_i^N f_i e_{ix}^k e_{iy}^l e_{iz}^m \tag{9}$$

and the central moments as

$$\tilde{\mu} x^k y^l z^m = \sum_i^N f_i (e_{ix} - u_x)^k \left(e_{iy} - u_y\right)^l (e_{iz} - u_z)^m \tag{10}$$

2.3 Turbulence modelling

The approach used for turbulence modelling is the Large Eddy Simulation (LES). This scheme introduces an additional viscosity, called turbulent eddy viscosity ν_t, in order to model the sub-grid turbulence. The LES scheme we have used is the Wall-Adapting Local Eddy viscosity model, that provides a consistent local eddy-viscosity and near wall behaviour (Ducros et al. 1998).

The actual implementation is formulated as follows:

$$\nu_t = \Delta_\mathrm{f}^2 \frac{\left(\mathrm{G}_{\alpha\beta}^\mathrm{d} \mathrm{G}_{\alpha\beta}^\mathrm{d}\right)^{\frac{3}{2}}}{\left(\mathrm{S}_{\alpha\beta} \mathrm{S}_{\alpha\beta}\right)^{\frac{5}{2}} + \left(\mathrm{G}_{\alpha\beta}^\mathrm{d} \mathrm{G}_{\alpha\beta}^\mathrm{d}\right)^{\frac{5}{4}}} \tag{11}$$

$$S_{\alpha\beta} = \frac{g_{\alpha\beta} + g_{\beta\alpha}}{2} \tag{12}$$

$$G_{\alpha\beta}^d = \frac{1}{2}\left(g_{\alpha\beta}^2 + g_{\beta\alpha}^2\right) - \frac{1}{3}\delta_{\alpha\beta} g_{\gamma\gamma}^2 \tag{13}$$

$$g_{\alpha\beta} = \frac{\partial u_\alpha}{\partial x_\beta} \tag{14}$$

where $\Delta_f = C_w \Delta x$ is the filter scale, S is the strain rate tensor of the resolved scales and the constant C_w is typically 0.325.

A generalized law of the wall that takes into account for the effect of adverse and favorable pressure gradients is used to model the boundary layer (Shih et al. 1999):

$$\frac{U}{u_c} = \frac{U_1 + U_2}{u_c} = \frac{u_\tau}{u_c}\frac{U_1}{u_\tau} + \frac{u_p}{u_c}\frac{U_2}{u_p} \tag{15}$$

$$= \frac{\tau_w}{\rho u_\tau^2}\frac{u_\tau}{u_c} f_1\left(y^+ \frac{u_\tau}{u_c}\right) + \frac{\mathrm{d}p_w/\mathrm{d}x}{|\mathrm{d}p_w/\mathrm{d}x|}\frac{u_p}{u_c} f_2\left(y^+ \frac{u_p}{u_c}\right) \tag{16}$$

$$y^+ = \frac{u_c y}{\nu} \tag{17}$$

$$u_c = u_\tau + u_p \tag{18}$$

$$u_\tau = \sqrt{|\tau_w|/\rho} \tag{19}$$

$$u_p = \left(\frac{\nu}{\rho}\left|\frac{\mathrm{d}p_w}{\mathrm{d}x}\right|\right)^{1/3}. \tag{20}$$

Here, y is the normal distance from the wall, u_τ is the skin friction velocity, τ_w is the turbulent wall shear stress, dp_w/dx is the wall pressure gradient, u_p is a characteristic velocity of the adverse wall pressure gradient and U is the mean velocity at a given distance from the wall. The interpolating functions f_1 and f_2 given by Shih et al. are depicted in **Error! Reference source not found.**Figure 2.

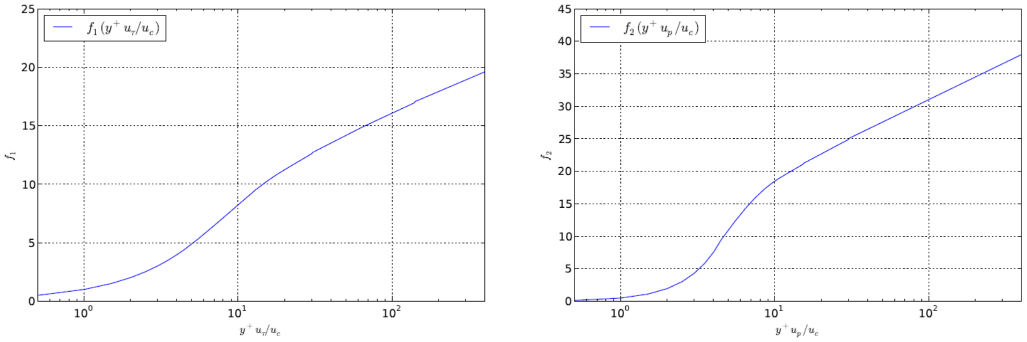

Figure 2: Unified laws of the wall

2.4 Treatment of moving geometries

The treatment of moving boundary conditions is straightforward and similar to the handling of fixed boundaries. In basic LBM implementations the wall boundary conditions for straight boundaries are typically implemented following a simple bounce-back rule for the no-slip boundary condition and a bounce-forward rule for the free-slip. In XFlow the statistical distribution functions f_i coming from the boundaries are reconstructed taking into account the wall distance, the velocity and the surface properties. The set of statistical distribution functions to be reconstructed is recomputed each time-step based on the updated position of the moving boundaries. A reference distance to the wall, velocity, surface orientation and curvatures are taken into account in order to solve the wall boundary condition.

As the physics are not implemented using surface elements, XFlow relaxes the requirements imposed to the geometries and it is tolerant to crossing or complex surfaces.

3: Simulations setup

The simulation of tests points by XFlow has been conducted in the virtual wind tunnel featured by the software, designed for external aerodynamics simulations. The size of the wind tunnel is set to 40x30x20 m and periodic boundary conditions are applied at the top and bottom boundaries, as well as at the lateral boundaries.

The required inputs to run the simulation are:

- D-JET model geometry (actual loft) with flow through inlet
- D-JET mass, centre of gravity and full inertia tensor at the test point time
- Test point airspeed, air density, temperature and dynamic viscosity
- Flight controls deflections corresponding to the test point, slightly reduced by a factor determined from static wind tunnel data validation where applicable.

The model is placed at the initial angular positions corresponding to the test point being evaluated, and its behaviour set to rigid body dynamics with the relevant Degrees Of Freedom (DOF). Once the simulation starts, no further input from flight test data is used by XFlow. The average setup time for these simulations in XFlow is approximately 15 min.

4: Flight test manoeuvres

This section presents the XFlow numerical results for the Diamond D-JET performing three types of flight test manoeuvres, namely: (i) pitch capture; (ii) Dutch roll; and (iii) stall. The performance of the CFD tool is evaluated by comparing its results with flight test data for the corresponding manoeuvres. Additionally, the ability of XFlow to simulate other kind of manoeuvres is illustrated with the D-JET spinning.

4.1 Pitch capture

This maneuver involves flight at a predetermined speed in trimmed conditions, aggressively pitching up five degrees for one or two seconds without re-trimming, then return to the trimmed condition with flight controls fixed. The pitch oscillation frequency and damping are resulting parameters used to qualify flight handling qualities.

Pitch capture is simulated with one degree of freedom in the pitch angle, starting at the flight test out of trim pitch angle at 0.7 seconds. The elevator deflection is preset to the trimmed condition as in flight test.

Figure 3 shows the pitch evolution of the D-JET for the given test conditions, where XFlow results are represented in orange and flight test data in black. As it is shown in the figure, numerical results yield a similar pitch response curve, although at higher frequency and lower damping than the experimental one.

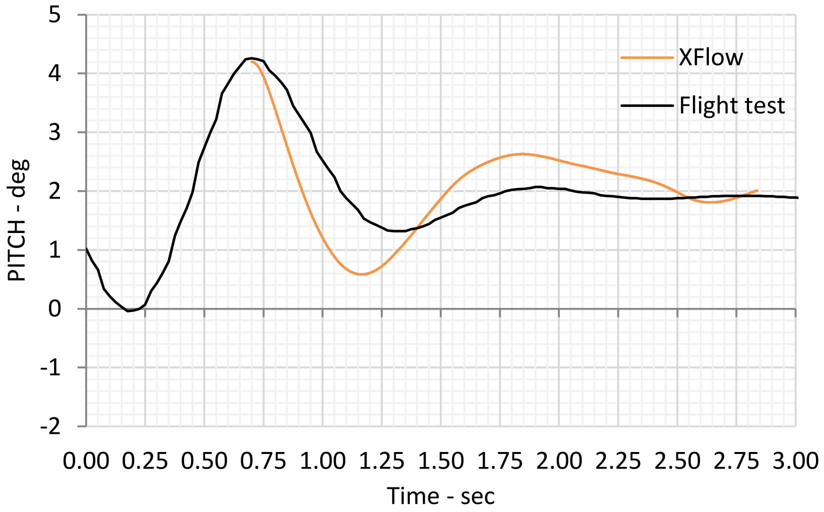

Figure 3: **Pitch capture simulation**

4.2 Dutch roll

Dutch roll is initiated in level flight with a rudder input to excite the Dutch roll motion, after which the flight controls are held fixed. The resulting yaw causes the aircraft to roll due to the dihedral effect, and subsequent oscillations in roll and pitch are analysed for frequency and damping. As with pitch capture, Dutch roll frequency and damping must meet specific requirements for acceptable flight handling characteristics.

Dutch roll is simulated by XFlow with three degrees of freedom: pitch, roll, and yaw. The elevator is set for trimmed conditions at 100 KIAS and 20500 ft. The simulation starts when the rudder is centred (7.6 seconds).

Figure 4 shows both the experimental and numerical results of this test. The agreement between simulation and flight test data is excellent, with a Dutch roll frequency only 9% above flight test. Damping is a match for the first oscillations. Similar results are obtained at higher speeds (up to 200 KIAS) with a slightly higher overestimate of the frequency, but still within 15%.

As shown in Figure 4, the bank angle at which the aircraft settles is a spiral stability effect which varies from one Dutch roll manoeuvre to the next, it is therefore expected that XFlow does not settle to the same bank angle.

This 13 seconds simulation was computed in 32 hours on a dual quad-core Xeon workstation. Simulations at coarser resolution have lower damping.

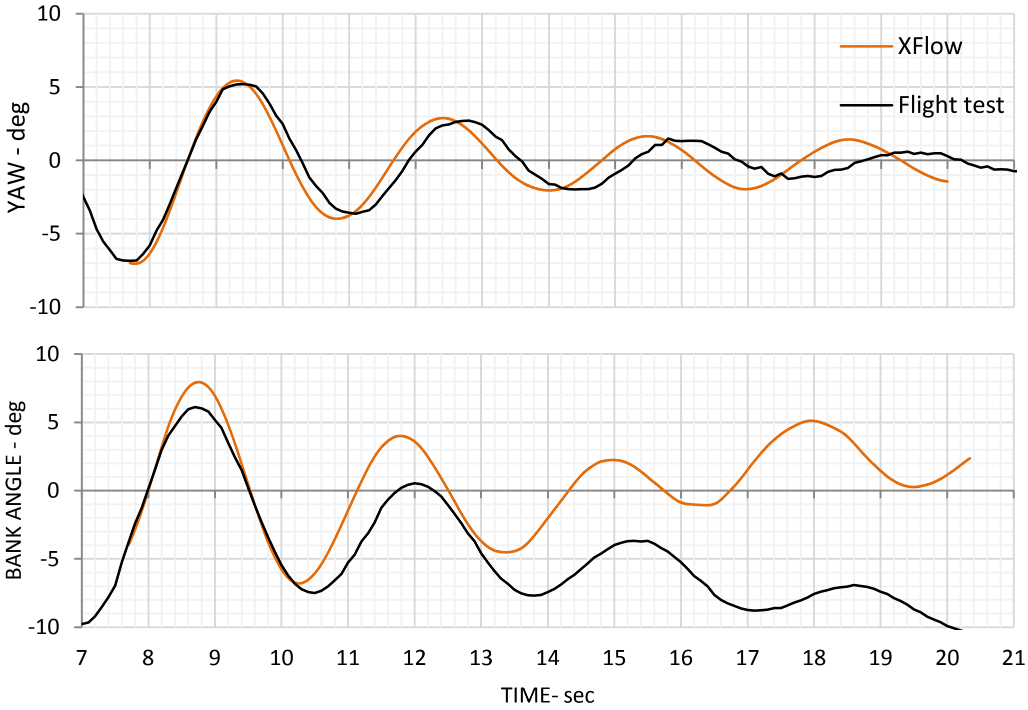

Figure 4: **Dutch roll simulation**

The Dutch roll manoeuvre is illustrated in Figure 5, where the position of the D-JET is captured in three different moments of the test. The images highlight the roll motion of the aircraft.

Figure 5: **Dutch roll**

4.3 Stall

The test point simulated here involves stall and post-stall behaviour at angle of attack approaching 30 degrees. When the angle of attack goes beyond 25 degrees, the pilot pushes the nose down as this represents a flight test limit. The aircraft is in a clean configuration (flaps and gear are retracted).

This simulation focuses on the evolution of the angle of attack in the post-stall regime, and the effectiveness of the elevator in bringing the nose of the aircraft down. Elevator deflection and airspeed are simulation inputs, the values of which are shown in Figure 6. The Angle of Attack (AOA) is the simulation output and it is shown in Figure 7.

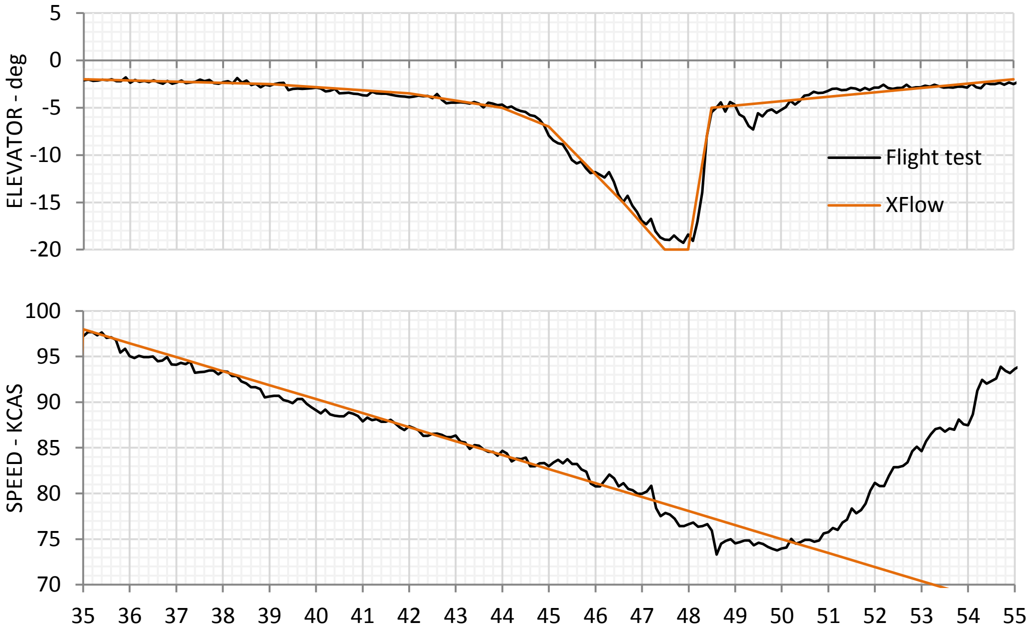

Figure 6: **Stall simulation inputs: Elevator deflection and airspeed**

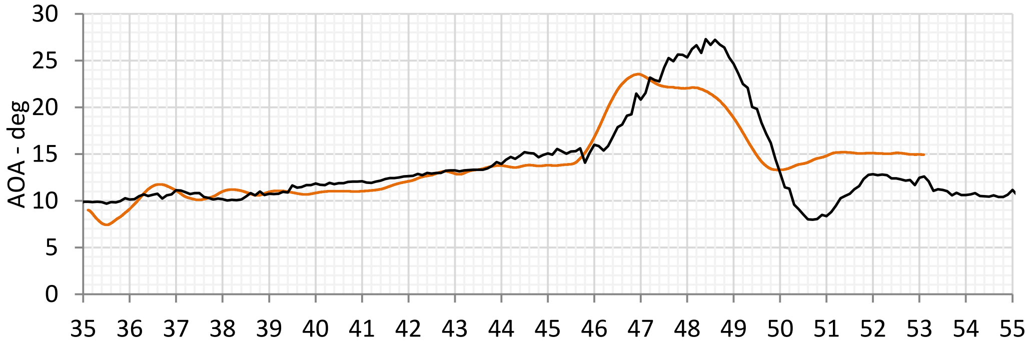

Figure 7: **Stall simulation output: Angle of attack**

From Figure 7 it can be stated that XFlow reasonably predicts the elevator effectiveness while the aircraft is fully stalled, though it underestimates the maximum angle of attack by 4 degrees.

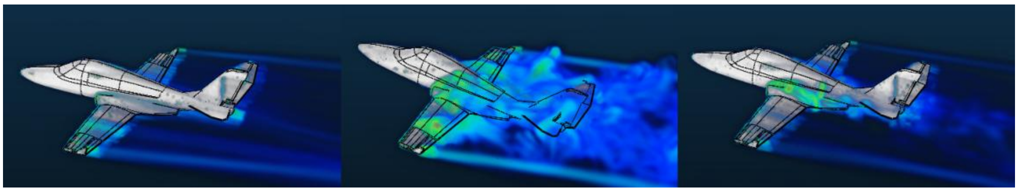

Figure 8: **Stall manoeuvre**

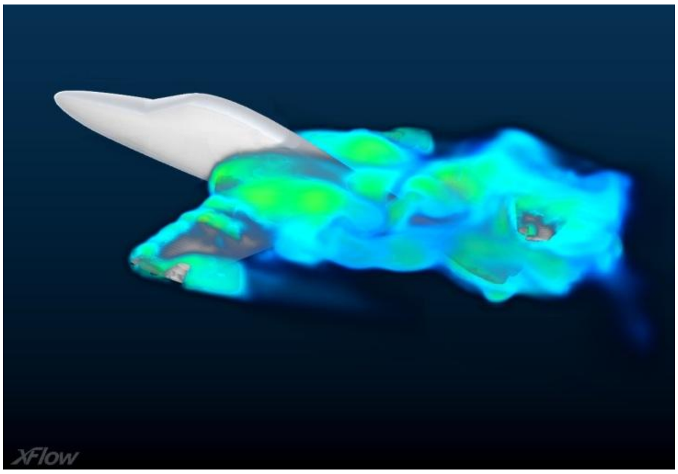

Figure 9: **Stall manoeuvre at maximum angle of attack**

Figures 8 and 9 show some images of the numerical stall test. The one shown in Figure 9 corresponds to the moment at which the D-JET reaches the maximum angle of attack; it can be observed how the horizontal tail is fully submerged in the turbulent flow.

4.4 Spin

Flight test data for the spin test of the D-JET is not available. Nonetheless, spin data has been obtained in a wind tunnel facility. For a specific set of conditions simulated by XFlow with pro-spin flight control deflections, the angle of attack stabilized at 47 degrees and corresponds to wind tunnel derived simulations conducted with D-Six (a Bihrle Applied Research simulation software). The spin rate was higher with XFlow.

As the flight test program of the D-JET progresses, more validation studies will be conducted with a variety of test conditions such as flight handling characteristics with ice shapes attached to the wing and tail leading edges.

Figure 10 shows an image of XFlow simulating a D-JET spin mode.

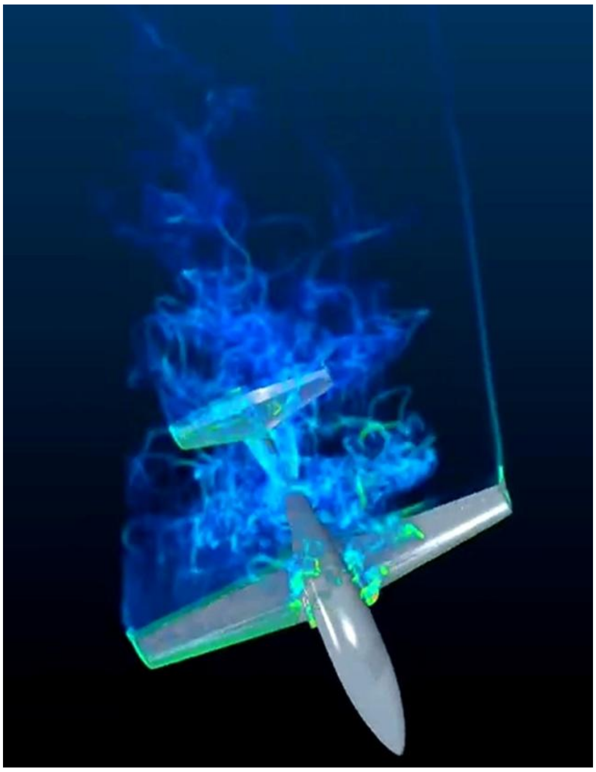

Figure 10: **Spin simulation**

5: Conclusions

XFlow offers the potential of reliably evaluating the flight handling characteristics of any aircraft configuration at the conceptual design stage, and can complement wind tunnel data with dynamic stability data – including power or propeller slipstream effects.

Indeed, a total of four flight manoeuvre simulations have been conducted with success by XFlow on the Diamond D-JET developed by Diamond Aircraft Industries in Canada: the pitch capture, the Dutch roll, the stall and spin simulation. The CFD setup and preparation for such cases is extremely short despite the complex fluid-structure interaction required to model such dynamics. Only a couple of mechanical inputs of the D-JET are required for the rigid body dynamics of the aircraft. No time-consuming re-meshing techniques are required due to the mesh-less approach of XFlow, adapting the fluid domain dynamically as the aircraft moves.

Considering the relatively good level of correlation with flight test data, XFlow can also be considered as a flight test risk mitigation tool by simulating a range of flight test manoeuvres such as deep stall and spins prior to actual testing. Further validation studies will determine its domain of validity.

REFERENCES

Asinari, P., 2008, *Entropic multiple-relaxation-time lattice Boltzmann models*, Tech. rep., Politecnico di Torino, Torino, Italy, 2008.

Chen, H., Chen, S., & Matthaeus, W., 1992, *Recovery of the Navier-Stokes equations using a lattice-gas Boltzmann method*, Physical Review A, vol. 45, pp. 5339.

Ducros, F., Nicoud, F., & Poinsot, T., 1998, *Wall-adapting local eddy-viscosity models for simulations in complex geometries*, Proceedings of 6th ICFD Conference on Numerical Methods for Fluid Dynamics, pp. 293-299.

Farhat, C., Pierson, K. & Degand, C., 2001, *Multidisciplinary Simulation of the Maneuvering of an Aircraft.* Engineering with Computers 17: 16-27.

Ghoreyshi, M., Vallespin, D., Da Ronch, A.,Badcockx, K. J., Vos, J. & Hitze, S., 2010, *Simulation of Aircraft Manoeuvres Based on Computational Fluid Dynamics.* American Institute of Aeronautics and Astronautics.

Hardy, J., Pomeau, Y., & de Pazzis, O., 1973, *Time evolution of a twodimensional model system. I. Invariant states and time correlation functions.* J. Math. Phys., 14(12):1746-1759.

Higuera, F.J., & Jimenez, J., 1989, *Boltzmann approach to lattice gas simulations*, Europhysics Letters, vol. 9, pp. 663-668.

Hines, D.O. ed., 2000, *Simulation in Support of Flight Testing*, Flight Test Techniques Series, RTO AG- 300 Volume 19, The Research and Technology Organization (RTO) of NATO.

Holman, D.M., Brionnaud, R.M., Martínez, F.J., & Mier-Torrecilla, M., 2012, *Advanced Aerodynamic Analysis of the NASA High-Lift Trap Wing with a Moving Flap Configuration.* 30th AIAA Applied Aerodynamics Conference, New Orleans, Louisiana, 25 - 28 June.

d'Humières, D., 2002, *Multiple-relaxation-time lattice Boltzmann models in three dimensions*, Philosophical Transactions of the Royal Society of London. Series A: Mathematical, Physical and Engineering Sciences, Vol. 360, No. 1792, 2002, pp. 437-451.

Johnson, A.A., 2006, *Dynamic-mesh CFD and its application to flapping-wing micro-air vehicles*, 25th Army Science Conference, Orlando.

Lemon, K.A., 2011, *Application of a six degrees of freedom adaptive controller to a general aviation aircraft*. MSc Thesis, Wichita State University.

Next Limit Technologies, 2013, XFlow, http://www.xflowcfd.com/

Premnath, K., & Banerjee, S., 2011, *On the Three-Dimensional Central Moment Lattice Boltzmann Method*, Journal of Statistical Physics, 2011, pp. 1-48.

Qian, Y.H., D'Humières, D., & Lallemand, P., 1992, *Lattice BGK models for Navier-Stokes equation*. EPL (Europhysics Letters), 17:479.

Ran, Z., & Xu, Y., 2008, *Entropy and weak solutions in the thermal model for the compressible Euler equations,* axXiv:0810.3477.

Shan, X., & Chen, H., 2007, *A general multiple-relaxation-time Boltzmann models in three dimensions,* International Journal of Modern Physics C, Vol. 18, No. 4, 2007, pp. 635-643.

Shih, T., Povinelli, L., Liu, N., Potapczuk, M., & Lumley, 1999, J., *A generalized wall function*, NASA Technical Report.

Shishkin, A. & Wagner, C., 2010, *Numerical modeling of flow dynamics induced by fruit flies during free-flight*, V European Conference on Computational Fluid Dynamics, ECCOMAS CFD 2010, Lisbon (Portugal), 14-17 June.